# Strapdown Inertial System Based on Improved MEMS Error Models

*Tsonyo Slavov, Petko Petkov*

*Department of Automatics, Technical University of Sofia, 1756 Sofia,*
*Emails: ts_slavov@tu-sofia.bg      php@tu-sofia.bg*

**Abstract:** *An algorithm for a low cost strapdown inertial navigation system based on improved MEMS error models and aided with a magnetometer and GPS sensor measurements is proposed. The system utilizes the Analog Devices tri-axial Inertial Measurement Unit ADIS16405 involving MEMS gyroscopes, accelerometers and magnetometers and implements Extended Kalman Filter of 22nd order. The main contribution is the usage of more accurate models of MEMS sensor noises which take into account not only the white noises and random walk terms but also the bias instabilities of the sensor noises.*

**Keywords:** *Strapdown navigation systems, Inertial systems, MEMS inertial sensors, Sensor noises, Extended Kalman Filter.*

## 1.  Introduction

The low cost strapdown inertial navigation systems of medium accuracy are widely utilized in robotics, control of unmanned air vehicles, personal transportation and many other applications [2, 4, 9]. The development of such systems is based on the implementation of Micro Electro Mechanical Systems (MEMS) gyroscopes and acce-lerometers characterized by the presence of significant noises in the output signals. The usual practice in modeling the sensor noises in low cost inertial systems is to take into account only the white noise terms and eventually random walk terms in order to reduce the order of the Kalman filter implemented. With the appearance of new powerful signal processors the volume of computational work

related to the implementation of Kalman filter does not present further a significant problem, which allows the use of more sophisticated sensor noise models thus improving the navigation system accuracy.

The aim of this paper is to investigate an algorithm for a low-cost strapdown inertial navigation system aided with a magnetometer and GPS sensor measurements based on improved MEMS error models. The system utilizes the Analog Devices tri-axial Inertial Measurement Unit (IMU) ADIS16405 involving MEMS gyroscopes, accelerometers and magnetometers. As shown earlier (see for instance [7]), the output signals of these sensors have noises which consist of bias instability, random walk and white noise terms. As usual, the attitude, velocity and body position are estimated by using an Extended Kalman Filter (EKF) implemented on digital signal processor. The main contribution of the paper is the usage of more accurate models of MEMS sensor noises which take into account not only the white noises and random walk terms but also the bias instabilities of the corresponding sensor noises. This leads to an EKF of 22nd order.

The content of the paper is as follows. In Section 2 we present a kinematic model of the navigation system under some reasonable assumptions. In Section 3 we derive an improved model of the inertial sensor noises which is incorporated into the system model in Section 4. The design of the Extended Kalman Filter is done in Section 5 and the full algorithm is presented in Section 6. The results from system simulation are presented in Section 7 and some conclusions are derived in Section 8.

The units for gyro and accelerometers noises used in the paper conform to the units used in [1].

## 2. Kinematic model of the navigation system

To determine the vehicle attitude, velocity and position in space we use the model of a rigid body with six degrees of freedom. The velocity and position of the vehicle are represented in the North-East-Down (NED) Earth fixed reference frame and the angular rate and linear acceleration are represented in a body fixed reference frame. In deriving the model we neglect the Earth rotation because the Earth rate is much smaller than the sensitivity of the gyro sensors used and we do not take into account the non-spherical shape of the Earth. The model equation thus obtained is [9]

$$(1) \qquad \begin{bmatrix} \dot{q} \\ \dot{V} \\ \dot{P} \end{bmatrix} = \begin{bmatrix} \frac{1}{2}\Omega(q)w \\ C_{be}a_s + \begin{bmatrix} 0 & 0 & g \end{bmatrix}^{\mathrm{T}} \\ V \end{bmatrix},$$

where $q$ is the unit quaternion vector

$$(2) \qquad q = \begin{bmatrix} a & b & c & d \end{bmatrix}^{\mathrm{T}},$$

$V$ is a vector containing the linear velocity components,

4

(3)
$$V = \begin{bmatrix} V_x & V_y & V_z \end{bmatrix}^{\mathrm{T}},$$

and the vector

$$P = \begin{bmatrix} P_x & P_y & P_z \end{bmatrix}^{\mathrm{T}}$$

contains the body position coordinates.

The matrix $C_{be}$ in (1) is the direction cosine matrix [2, 9] which gives the relationship between vectors in the body fixed reference frame and the corresponding vectors in the Earth fixed reference frame. This matrix has the form

(4)
$$C_{be} = \begin{bmatrix} c_{11} & c_{12} & c_{13} \\ c_{21} & c_{22} & c_{23} \\ c_{31} & c_{32} & c_{33} \end{bmatrix},$$

where the elements of $C_{be}$ are given by [9]:

$$c_{11} = a^2 + b^2 - c^2 - d^2,$$
$$c_{12} = 2(bc - ad),$$
$$c_{13} = 2(bd + ac),$$
$$c_{21} = 2(bc + ad),$$
$$c_{22} = a^2 - b^2 + c^2 - d^2,$$
$$c_{23} = 2(cd - ab),$$
$$c_{31} = 2(bd - ac),$$
$$c_{32} = 2(cd + ab),$$
$$c_{33} = a^2 - b^2 - c^2 + d^2.$$

The matrix $C_{be}$ in (4) is orthogonal so that

(5)
$$C_{eb} = C_{be}^{-1} = C_{be}^{\mathrm{T}}$$

where the matrix $C_{eb}$ gives the relationship between vectors in the Earth fixed reference frame and the corresponding vectors in the body fixed reference frame. The matrix $\Omega(q)$ is determined by the expression

(6)
$$\Omega(q) = \begin{bmatrix} -b & -c & -d \\ a & -d & c \\ d & a & -b \\ -c & b & a \end{bmatrix},$$

and

(7)
$$w = \begin{bmatrix} w_x & w_y & w_z \end{bmatrix}^{\mathrm{T}}$$

is the vector of true angular rates measured in the body fixed reference frame. The full acceleration, expressed in the body fixed frame, is represented as the sum

$$a_\mathrm{f} = a_\mathrm{s} + C_\mathrm{eb}\begin{bmatrix} 0 & 0 & g \end{bmatrix}^\mathrm{T}$$

where $a_\mathrm{s} = [a_x \quad a_y \quad a_z]^\mathrm{T}$ is the specific acceleration and $g$ is the Earth's gravitational acceleration, computed for the given latitude. Note that the accelerometers can measure only the components of the specific acceleration $a_\mathrm{s}$.

After introducing the state variables

$$x_1 = a, \quad x_2 = b, \quad x_3 = c, \quad x_4 = d, \quad x_5 = V_x,$$
$$x_6 = V_y, \quad x_7 = V_z, \quad x_8 = P_x, \quad x_9 = P_y, \quad x_{10} = P_z,$$

the state space description of model (1) is obtained as

$$(8) \quad \dot{x} = \begin{bmatrix} \dot{x}_1 \\ \dot{x}_2 \\ \dot{x}_3 \\ \dot{x}_4 \\ --- \\ \dot{x}_5 \\ \dot{x}_6 \\ \dot{x}_7 \\ --- \\ \dot{x}_8 \\ \dot{x}_9 \\ \dot{x}_{10} \end{bmatrix} = \begin{bmatrix} -\dfrac{1}{2}x_2 w_x - \dfrac{1}{2}x_3 w_y - \dfrac{1}{2}x_4 w_z \\ \dfrac{1}{2}x_1 w_x - \dfrac{1}{2}x_4 w_y + \dfrac{1}{2}x_3 w_z \\ \dfrac{1}{2}x_4 w_x + \dfrac{1}{2}x_1 w_y - \dfrac{1}{2}x_2 w_z \\ -\dfrac{1}{2}x_3 w_x + \dfrac{1}{2}x_2 w_y + \dfrac{1}{2}x_1 w_z \\ --- \\ (x_1^2 + x_2^2 - x_3^2 - x_4^2)a_x + 2(x_2 x_3 - x_1 x_4)a_y + 2(x_2 x_4 + x_1 x_3)a_z \\ 2(x_2 x_3 + x_1 x_4)a_x + (x_1^2 - x_2^2 + x_3^2 - x_4^2)a_y + 2(x_3 x_4 - x_1 x_4)a_z \\ 2(x_2 x_4 - x_1 x_3)a_x + 2(x_3 x_4 + x_1 x_2)a_y + (x_1^2 - x_2^2 - x_3^2 + x_4^2)a_z + g \\ --- \\ x_5 \\ x_6 \\ x_7 \end{bmatrix}.$$

In equations (1) and (8) the input variables are the non-measurable exact rate $w$ and the non-measurable true specific acceleration $a_\mathrm{s}$, which makes these equations inappropriate for Kalman filter design. The measurable signals are the angular rate $w_\mathrm{m}$, measured by the gyros and the specific acceleration $a_\mathrm{m}$, measured by the accelerometers. These signals involve sensor noises which are investigated in the next Section.

6

## 3. Noise models of the inertial sensors

In the case under consideration the measurement of the angular rates and linear accelerations in the body fixed reference frame is done by using tri-axial MEMS gyroscopes and accelerometers combined with a tri-axial magnetometer in an Inertial Measurement Unit. For this aim we make use of the miniature IMU ADIS16405 (Fig. 1) [1].



Fig. 1. Inertial Measurement Unit ADIS16405

The gyros output $w_{\mathrm{m}}$ is expressed as

(9)
$$w_{\mathrm{m}} = w + b_w + \eta_w,$$

where $b_w$ is the gyro noise bias vector and $\eta_w$ is the angular random walk vector. Each component of the gyro noise bias

(10)
$$b_w = \begin{bmatrix} b_{wx} & b_{wy} & b_{wz} \end{bmatrix}^{\mathrm{T}}$$

is modeled as a sum of two components – bias instability and rate random walk [4, 7], so that

(11)
$$b_{wx} = x_{11} + x_{12}, \; b_{wy} = x_{13} + x_{14}, \; b_{wz} = x_{15} + x_{16},$$

where $x_{11}$, $x_{12}$, $x_{13}$, $x_{14}$, $x_{15}$, $x_{16}$ are solutions of the following differential equations:

(12)
$$\dot{x}_{11} = -\frac{1}{T_{\mathrm{g}}} x_{11} + \frac{K_{g_1}}{T_{\mathrm{g}}} w_{w_1},$$

$$\dot{x}_{12} = K_{g_2} w_{w_2}$$

$$\dot{x}_{13} = -\frac{1}{T_{\mathrm{g}}} x_{13} + \frac{K_{g_1}}{T_{\mathrm{g}}} w_{w_4},$$

$$\dot{x}_{14} = K_{g_2} w_{w_5},$$

$$\dot{x}_{15} = -\frac{1}{T_{\mathrm{g}}} x_{15} + \frac{K_{g_1}}{T_{\mathrm{g}}} w_{w_7},$$

$$\dot{x}_{16} = K_{g_2} w_{w_8},$$

$T_g$ is a time constant, $K_{g_1}$, $K_{g_2}$ are constants and $w_{w_1}$, $w_{w_2}$, $w_{w_4}$, $w_{w_5}$, $w_{w_7}$, $w_{w_8}$ are white noises with unit variances.

The angular random walk vector is given by

$$(13) \qquad \eta_w = \begin{bmatrix} \eta_{w_x} \\ \eta_{w_y} \\ \eta_{w_z} \end{bmatrix} = \begin{bmatrix} K_{g_3} w_{w_3} \\ K_{g_3} w_{w_6} \\ K_{g_3} w_{w_9} \end{bmatrix}$$

where $K_{g_3}$ is a constant and $w_{w_3}$, $w_{w_6}$, $w_{w_9}$ are white noises with unit variance.

In a similar way the measured specific acceleration $a_m$ is determined as

$$(14) \qquad a_m = a_s + b_a + \eta_a,$$

where $b_a$ is the vector of three-axis accelerometer bias and $\eta_a$ is the vector of velocity random walks. Each component of the accelerometer bias

$$b_a = \begin{bmatrix} b_{ax} & b_{ay} & b_{az} \end{bmatrix}^T$$

is expressed as a sum of bias instability and acceleration random walk,

$$(15) \qquad b_{ax} = x_{17} + x_{18}, \; b_{ay} = x_{19} + x_{20}, \; b_{az} = x_{21} + x_{22},$$

where $x_{17}$, $x_{18}$, $x_{19}$, $x_{20}$, $x_{21}$, $x_{22}$ are solutions of the differential equations

$$(16) \qquad \begin{aligned} \dot{x}_{17} &= -\frac{1}{T_a} x_{17} + \frac{K_{a_1}}{T_a} w_{a_1}, \\ \dot{x}_{18} &= K_{a_2} w_{a_2}, \\ \dot{x}_{19} &= -\frac{1}{T_a} x_{19} + \frac{K_{a_1}}{T_a} w_{a_4}, \\ \dot{x}_{20} &= K_{a_2} w_{a_5}, \\ \dot{x}_{21} &= -\frac{1}{T_a} x_{21} + \frac{K_{a_1}}{T_a} w_{a_7}, \\ \dot{x}_{22} &= K_{a_2} w_{a_8}, \end{aligned}$$

$T_a$ is a time constants, $K_{a_1}$, $K_{a_2}$ are constants, and $w_{a_1}$, $w_{a_2}$, $w_{a_4}$, $w_{a_5}$, $w_{a_7}$, $w_{a_8}$ are white noises with unit variances.

The velocity random walk vector is determined from

$$(17) \qquad \eta_a = \begin{bmatrix} \eta_{a_x} \\ \eta_{a_y} \\ \eta_{a_z} \end{bmatrix} = \begin{bmatrix} K_{a_3} w_{a_3} \\ K_{a_3} w_{a_6} \\ K_{a_3} w_{a_9} \end{bmatrix},$$

where $K_{a_3}$ is a constant, and $w_{a_3}$, $w_{a_6}$, $w_{a_9}$ are white noises with unit variances.

The noise model of the inertial unit ADIS16405, described by the equations (9)-(17), is determined by using the methodology presented in [7]. The model parameters are computed by a least-squares method minimizing the integral of the quadratic error representing the difference between the spectral density of the model

8

and the spectral density of the actual noise. The power spectral density of the noise is determined on the basis of 1 000 000 measurements for a fixed inertial unit. The power spectral densities of the model noises and actual gyro and accelerometer noises are shown in Figs 2 and 3, respectively. The model parameters obtained are shown in Table 1. The model of the magnetometer noises is discussed later in Section 4.

Table 1. Noise model parameters of gyroscopes and accelerometers

| Gyroscopes | | | | Accelerometers | | | |
|---|---|---|---|---|---|---|---|
| $T_g$ | $K_{g_1} \times \dfrac{180}{\pi}$, rad | $K_{g_2} \times \dfrac{180}{\pi}$, rad | $K_{g_3} \times \dfrac{180}{\pi}$, rad | $T_a$ | $K_{a_1}$ | $K_{a_2}$ | $K_{a_3}$ |
| 36.041 | 0.869087 | $6.42582 \times 10^{-3}$ | 0.382397 | 3.95616 | $7.941589 \times 10^{-3}g$ | $4.29474 \times 10^{-4}g$ | $3.45394g$ |
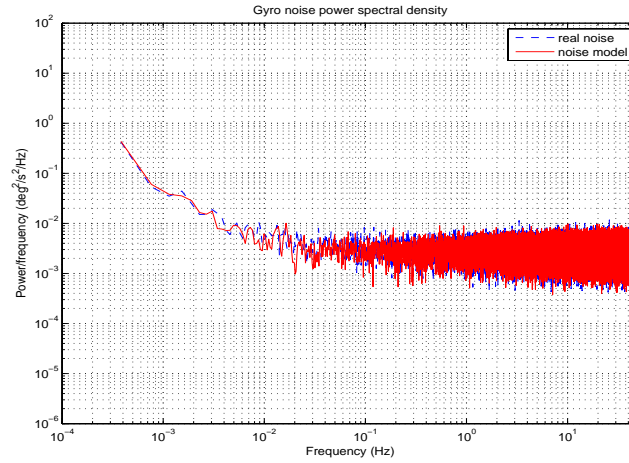


Fig. 2. Power spectral density of gyro noise
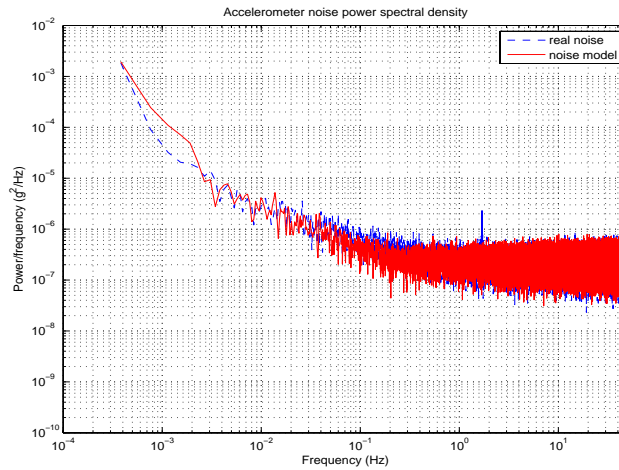


Fig. 3. Power spectral density of accelerometer noise

9

## 4. Navigation system model incorporating sensor noises

Taking into account (9) and (14), the measurement vector is obtained as

$$(18) \qquad u = \begin{bmatrix} w_{\mathrm{m}} \\ a_{\mathrm{m}} \end{bmatrix} = \begin{bmatrix} w + b_w + \eta_w \\ a_{\mathrm{s}} + b_{\mathrm{a}} + \eta_{\mathrm{a}} \end{bmatrix}.$$

In order to use the measured variables instead of true variables we shall implement the approach presented in [8]. After solving (18) with respect to the true angular rate and specific acceleration one obtains

$$(19) \qquad \begin{aligned} w &= w_{\mathrm{m}} - b_w - \eta_w \\ a_{\mathrm{s}} &= a_{\mathrm{m}} - b_{\mathrm{a}} - \eta_{\mathrm{a}} \end{aligned}.$$

Substituting (19) in (1) and extending (8) with the equations of gyro and accelerometer biases, the vehicle attitude, velocity and position are described by the nonlinear model от 22nd order

$$(20) \qquad f(x, \eta, u) = \begin{bmatrix} \dot{q} \\ \dot{V} \\ \dot{P} \\ \dot{b}_w \\ \dot{b}_{\mathrm{a}} \end{bmatrix} = \begin{bmatrix} \dfrac{1}{2}\Omega(q)(w_{\mathrm{m}} - b_w - \eta_w) \\ C_{\mathrm{be}}(q)(a_{\mathrm{m}} - b_{\mathrm{a}} - \eta_{\mathrm{a}}) + \begin{bmatrix} 0 & 0 & g \end{bmatrix}^{\mathrm{T}} \\ V \\ f_w(b_w, w_w) \\ f_{\mathrm{a}}(b_{\mathrm{a}}, w_{\mathrm{a}}) \end{bmatrix},$$

$$w_w = \begin{bmatrix} w_{w_1} & w_{w_2} & w_{w_3} & w_{w_4} & w_{w_5} & w_{w_6} & w_{w_7} & w_{w_8} & w_{w_9} \end{bmatrix}^{\mathrm{T}}$$

$$w_{\mathrm{a}} = \begin{bmatrix} w_{\mathrm{a}_1} & w_{\mathrm{a}_2} & w_{\mathrm{a}_3} & w_{\mathrm{a}_4} & w_{\mathrm{a}_5} & w_{\mathrm{a}_6} & w_{\mathrm{a}_7} & w_{\mathrm{a}_8} & w_{\mathrm{a}_9} \end{bmatrix}^{\mathrm{T}},$$

$$\eta = \begin{bmatrix} w_w & w_{\mathrm{a}} \end{bmatrix}^{\mathrm{T}},$$

where $f_w$ and $f_{\mathrm{a}}$ are the right hand sides of the differential equations (12) and (16) for the gyro and accelerometer biases, respectively. The state vector is defined as

$$x = [x_1 \ x_2 \ x_3 \ x_4 \ x_5 \ x_6 \ x_7 \ x_8 \ x_9 \ x_{10} \ x_{11} \ x_{12} \ x_{13} \ x_{14} \ x_{15} \ x_{16} \ x_{17} \ x_{18} \ x_{19} \ x_{20} \ x_{21} \ x_{22}].$$

The elements of the vector $\eta$ are non-correlated white noises with zero means and unit variances. Thus, for the variance matrix of noise $\eta$ one obtains

$$(21) \qquad Q = I_{18},$$

where $I_{18}$ is the 18×18 unit matrix. The equations (20) describe completely the kinematic of the six degrees of freedom rigid body and in contrast to equation (1), are functions of the measurable angular rates and specific accelerations.

As noted in Section 1, the inertial navigation system is aided with measurements from GPS and tri-axial magnetometers which allow to improve the accuracy of the updated estimate produced by a Kalman filter. That is why the model of the output signals is given by

$$(22) \qquad z = y + v, \quad y = h(x) = \begin{bmatrix} B_{\mathrm{b}} \\ V_{\mathrm{GPS}} \\ P_{\mathrm{GPS}} \end{bmatrix} = \begin{bmatrix} C_{\mathrm{eb}}(q)B_{\mathrm{e}} \\ V_{\mathrm{GPS}} \\ P_{\mathrm{GPS}} \end{bmatrix},$$

where $B_b$ is the vector of magnetic field measurements in the body fixed reference frame, $B_e$ is the magnetic field vector in the Earth fixed reference frame, $V_{GPS}$ and $P_{GPS}$ are the linear velocities and positions, respectively, measured by a GPS sensor and

(23)
$$v = \left[ v_{Bx} \quad v_{By} \quad v_{Bz} \quad v_{Vx} \quad v_{Vy} \quad v_{Vz} \quad v_{Px} \quad v_{Py} \quad v_{Pz} \right]^{\mathrm{T}}$$

is a vector that consists of magnetometer measurement noises ($v_{Bx}, v_{By}, v_{Bz}$) and GPS measurement noises ($v_{Vx}, v_{Vy}, v_{Vz}, v_{Px}, v_{Py}, v_{Pz}$). It is assumed that the elements of (23) are non-correlated white noises with zero means and the variance matrix of $v$ is

$$R = \mathrm{diag}(Dv_{Bx}, Dv_{By}, Dv_{Bz}, Dv_{Vx}, Dv_{Vy}, Dv_{Vz}, Dv_{Px}, Dv_{Py}, Dv_{Pz}),$$

where the diagonal elements of $R$ are equal to the variances of the corresponding components of $v$. In equation (22) the magnetic field in the body fixed frame is expressed as a function of the constant magnetic field in the Earth fixed reference frame by using the inverse of direction cosine matrix.

## 5. Design of an extended Kalman filter

After discretization of equation (20) with first order right differences one obtains
(24) $\quad x_k = \Phi(x_{k-1}, \eta_{k-1}, u_{k-1}), \quad \Phi(x_{k-1}, \eta_{k-1}, u_{k-1}) = f(x_{k-1}, \eta_{k-1}, u_{k-1})T_0 + x_{k-1},$
where $T_0 = 0.01$ s is the sampling period. Equations (22) and (24) are used in the design of a discrete Extended Kalman Filter (EKF) [3]. The EKF equation to predict the state estimation is
(25)
$$\hat{x}_k(+) = \hat{x}_k(-) + K_{\mathrm{EKF}_k}(z_k - \hat{y}_k),$$

where

$$\hat{x}_k(+) = \left[\hat{a}_k \quad \hat{b}_k \quad \hat{c}_k \quad \hat{d}_k \quad \hat{V}_{x_k} \quad \hat{V}_{y_k} \quad \hat{V}_{z_k} \quad \hat{P}_{x_k} \quad \hat{P}_{y_k} \quad \hat{P}_{z_k} \quad \hat{b}_{wx_k} \quad \hat{b}_{wy_k} \quad \hat{b}_{wz_k} \quad \hat{b}_{ax_k} \quad \hat{b}_{ay_k} \quad \hat{b}_{az_k}\right]^{\mathrm{T}}$$

is a vector containing the state estimates of (24). The estimate $\hat{x}_k(-)$ is determined from

(26)
$$\hat{x}_k(-) = \hat{x}_{k-1}(+) + \int_{t_{k-1}}^{t_k} f(\hat{x}_{k-1}(+), u_{k-1})dt,$$

and the predicted output $\hat{y}_k$ is found from
(27)
$$\hat{y}_k = h(\hat{x}_k(-)).$$

The EKF gain $K_{\mathrm{EKF}_k}$ is obtained from [3, 8]

(28)
$$K_{\mathrm{EKF}_k} = P_k(-)H_k^{\mathrm{T}}[H_k P_k(-)H_k^{\mathrm{T}} + R]^{-1},$$

where the matrix $H_k$ is given by

(29)
$$H_k = \left.\frac{\partial h}{\partial x}\right|_{x=\hat{x}_k(-)}.$$

The apriori covariance matrix $P_k(-)$ is determined from

(30)
$$P_k(-) = F_{k-1}P_{k-1}(+)F_{k-1}^{\mathrm{T}} + T_0^2 G_{k-1}QG_{k-1}^{\mathrm{T}},$$

where

(31)
$$F_{k-1} = \frac{\partial \Phi}{\partial x}\bigg|_{x=\hat{x}_{k-1}(+),\eta_{k-1}=0} \quad , \quad G_{k-1} = \frac{\partial \Phi}{\partial u}\bigg|_{x=\hat{x}_{k-1}(+),\eta_{k-1}=0} .$$

The aposteriori covariance matrix $P_k(+)$ is determined as

(32)
$$P_k(+) = [I_{22} - K_{\mathrm{EKF}_k}H_k]P_k(-),$$

where $I_{22}$ is the 22×22 unit matrix. It is seen from equations (28), (30) and (32) that the determination of covariance matrices requires computation of the partial derivatives (29) and (31). After differentiation of $\Phi$ according to (31) one obtains

(33)
$$F = \frac{\partial \Phi}{\partial x} = \begin{bmatrix} F_{qq} & O_{4\times 3} & O_{4\times 3} & F_{qb_w} & O_{4\times 6} \\ F_{Vq} & O_{3\times 3} & O_{3\times 3} & O_{3\times 6} & F_{Vb_a} \\ O_{3\times 4} & F_{PV} & O_{3\times 3} & O_{3\times 6} & O_{3\times 6} \\ O_{6\times 4} & O_{6\times 3} & O_{6\times 3} & F_{b_w b_w} & O_{6\times 6} \\ O_{6\times 4} & O_{6\times 3} & O_{6\times 3} & O_{6\times 6} & F_{b_a b_a} \end{bmatrix} T_0 + I_{22},$$

where

$$F_{qq} = \frac{1}{2}\begin{bmatrix} 0 & -w_x & -w_y & -w_z \\ w_x & 0 & w_z & -w_y \\ w_y & -w_z & 0 & w_x \\ w_z & w_y & -w_x & 0 \end{bmatrix}, \quad F_{Vq} = \begin{bmatrix} F_{Va} & F_{Vb} & F_{Vc} & F_{Vd} \\ -F_{Vd} & -F_{Vc} & F_{Vb} & F_{Va} \\ F_{Vc} & -F_{Vd} & -F_{Va} & F_{Vb} \end{bmatrix},$$

$$\begin{aligned} F_{Va} &= 2(a.a_x - d.a_y + c.a_z) \\ F_{Vb} &= 2(b.a_x + c.a_y + d.a_z) \\ F_{Vc} &= 2(-c.a_x + b.a_y + a.a_z) \\ F_{Vd} &= 2(-d.a_x - a.a_y + b.a_z) \end{aligned}, \quad F_{qb_w} = \frac{1}{2}\begin{bmatrix} b & b & c & c & d & d \\ -a & -a & d & d & -c & -c \\ -d & -d & -a & -a & b & b \\ c & c & -b & -b & -a & -a \end{bmatrix},$$

$$F_{Vb_a} = \begin{bmatrix} -c_{11} & -c_{11} & -c_{12} & -c_{12} & -c_{13} & -c_{13} \\ -c_{21} & -c_{21} & -c_{22} & -c_{22} & -c_{23} & -c_{23} \\ -c_{31} & -c_{31} & -c_{32} & -c_{32} & -c_{33} & -c_{33} \end{bmatrix}, \quad F_{PV} = \begin{bmatrix} 1 & 0 & 0 \\ 0 & 1 & 0 \\ 0 & 0 & 1 \end{bmatrix},$$

$$F_{b_w b_w} = \begin{bmatrix} -\frac{1}{T_g} & 0 & 0 & 0 & 0 & 0 \\ 0 & 0 & 0 & 0 & 0 & 0 \\ 0 & 0 & -\frac{1}{T_g} & 0 & 0 & 0 \\ 0 & 0 & 0 & 0 & 0 & 0 \\ 0 & 0 & 0 & 0 & -\frac{1}{T_g} & 0 \\ 0 & 0 & 0 & 0 & 0 & 0 \end{bmatrix}, \quad F_{b_a b_a} = \begin{bmatrix} -\frac{1}{T_a} & 0 & 0 & 0 & 0 & 0 \\ 0 & 0 & 0 & 0 & 0 & 0 \\ 0 & 0 & -\frac{1}{T_a} & 0 & 0 & 0 \\ 0 & 0 & 0 & 0 & 0 & 0 \\ 0 & 0 & 0 & 0 & -\frac{1}{T_a} & 0 \\ 0 & 0 & 0 & 0 & 0 & 0 \end{bmatrix}.$$

The matrix $G$ is found as

12

$$(34) \qquad G = \frac{\partial \Phi}{\partial u} = \begin{bmatrix} f_{qw_g} & O_{4\times 9} \\ O_{3\times 9} & f_{Vw_a} \\ O_{3\times 9} & O_{3\times 9} \\ f_{w_g w_g} & O_{6\times 9} \\ O_{6\times 9} & f_{w_a w_a} \end{bmatrix},$$

where

$$f_{qw_g} = \frac{1}{2} \begin{bmatrix} 0 & 0 & K_{g_3} b & 0 & 0 & K_{g_3} c & 0 & 0 & K_{g_3} d \\ 0 & 0 & -K_{g_3} a & 0 & 0 & K_{g_3} d & 0 & 0 & -K_{g_3} c \\ 0 & 0 & -K_{g_3} d & 0 & 0 & -K_{g_3} a & 0 & 0 & K_{g_3} b \\ 0 & 0 & K_{g_3} c & 0 & 0 & -K_{g_3} b & 0 & 0 & -K_{g_3} a \end{bmatrix},$$

$$f_{Vw_a} = \begin{bmatrix} 0 & 0 & -K_{a_3} c_{11} & 0 & 0 & -K_{a_3} c_{12} & 0 & 0 & -K_{a_3} c_{13} \\ 0 & 0 & -K_{a_3} c_{21} & 0 & 0 & -K_{a_3} c_{22} & 0 & 0 & -K_{a_3} c_{23} \\ 0 & 0 & -K_{a_3} c_{31} & 0 & 0 & -K_{a_3} c_{32} & 0 & 0 & -K_{a_3} c_{33} \end{bmatrix},$$

$$f_{w_g w_g} = \begin{bmatrix} \dfrac{K_{g_1}}{T_g} & 0 & 0 & 0 & 0 & 0 & 0 & 0 & 0 \\ 0 & K_{g_2} & 0 & 0 & 0 & 0 & 0 & 0 & 0 \\ 0 & 0 & 0 & \dfrac{K_{g_1}}{T_g} & 0 & 0 & 0 & 0 & 0 \\ 0 & 0 & 0 & 0 & K_{g_2} & 0 & 0 & 0 & 0 \\ 0 & 0 & 0 & 0 & 0 & 0 & \dfrac{K_{g_1}}{T_g} & 0 & 0 \\ 0 & 0 & 0 & 0 & 0 & 0 & 0 & K_{g_2} & 0 \end{bmatrix},$$

$$f_{w_a w_a} = \begin{bmatrix} \dfrac{K_{a_1}}{T_a} & 0 & 0 & 0 & 0 & 0 & 0 & 0 & 0 \\ 0 & K_{a_2} & 0 & 0 & 0 & 0 & 0 & 0 & 0 \\ 0 & 0 & 0 & \dfrac{K_{a_1}}{T_a} & 0 & 0 & 0 & 0 & 0 \\ 0 & 0 & 0 & 0 & K_{a_2} & 0 & 0 & 0 & 0 \\ 0 & 0 & 0 & 0 & 0 & 0 & \dfrac{K_{a_1}}{T_a} & 0 & 0 \\ 0 & 0 & 0 & 0 & 0 & 0 & 0 & K_{a_2} & 0 \end{bmatrix}.$$

After differentiation of $h$ according to (29) one finds

$$(35) \qquad H = \frac{\partial h}{\partial x} = \begin{bmatrix} H_{Bq} & O_{3\times3} & O_{3\times3} & O_{3\times6} & O_{3\times6} \\ O_{3\times4} & I_{3\times3} & O_{3\times3} & O_{3\times6} & O_{3\times6} \\ O_{3\times4} & O_{3\times3} & I_{3\times3} & O_{3\times6} & O_{3\times6} \end{bmatrix},$$

where

$$H_{Bq} = \begin{bmatrix} H_{Ba} & H_{Bb} & H_{Bc} & H_{Bd} \\ H_{Bd} & -H_{Bc} & H_{Bb} & -H_{Ba} \\ -H_{Bc} & -H_{Bd} & H_{Ba} & H_{Bb} \end{bmatrix}, \qquad \begin{aligned} H_{Ba} &= 2(aB_{ex} + dB_{ey} - cB_{ez}) \\ H_{Bb} &= 2(bB_{ex} + cB_{ey} + dB_{ez}) \\ H_{Bc} &= 2(-cB_{ex} + bB_{ey} - aB_{ez}) \\ H_{Bd} &= 2(-dB_{ex} + aB_{ey} + bB_{ez}) \end{aligned} .$$

## 6. Algorithm of the navigation system aided with a GPS and magnetometer measurements

The pseudo code of the navigation system algorithm involves the following steps:

**Step 1.** The estimate $\hat{x}_k(-)$ is determined from equation (26) performing numerical integration by the fourth-order Runge-Kutta method.

**Step 2.** Normalize the quaternion dividing its elements by $\sqrt{a^2 + b^2 + c^2 + d^2}$ .

**Step 3.** Compute the matrices $F$ and $G$ according to (31), (33) and (34).

**Step 4.** Determine the apriori covariance matrix $P_k(-)$ from equation (30)

**Step 5.** Compute the matrix $H$ according to (29) and (35).

**Step 6.** Compute the predicted value of the output according to (27).

**Step 7.** Compute the EKF gain $K_{EKF}$ according to (28).

**Step 8.** Compute the current state estimate $\hat{x}_k(+)$ according to (25).

**Step 9.** Normalize the quaternion.

## 7. Navigation system simulation

The efficiency and accuracy of the navigation system combining measurements from MEMS gyros, accelerometers and magnetometers along with measurements from a GPS sensor is tested by several simulated experiments. For this aim a software environment working in MATLAB and Simulink is developed. The sample period of the navigation system is chosen as 0.01s. To simulate the GPS signals an S-function is developed, which implements the model (20) for zero values of the gyro and accelerometer noises. The output signals of this S-function are mixed with non-correlated white noises with zero means and variances

$$Dv_{V_x} = Dv_{Vy} = Dv_{Vz} = 5 , \; Dv_{P_X} = Dv_{Py} = 5, Dv_{P_Z} = 25 .$$

14

The values of these variances are chosen according to the practical data for GPS noises. These noises have significant variances and zero means while the output noises of the MEMS sensors are colored noises with significant biases. In the simulation we assume that the sampling period of GPS signals is 0.25 s. To simulate the exact body attitude we make use of the same S-function with exact outputs. The magnetometer outputs are obtained as

(36) $$B_b = C_{eb}(q)B_e + v_B,$$

where $v_B = \begin{bmatrix} v_{B_x} & v_{By} & v_{Bz} \end{bmatrix}^T$ are non-correlated white noises with zero means and variances

$$Dv_{B_X} = Dv_{B_y} = Dv_{Bz} = 0.005.$$

The components of the vector $B_e$ for the latitude of the city of Sofia are [6]

$$B_{ex} = 0.237744 \text{ G},$$
$$B_{ey} = 0.017658 \text{ G},$$
$$B_{ez} = 0.409335 \text{ G}.$$

The initial orientation of the system is NED (the axis $x_b$ points to North, the axis $y_b$ points to East and the axis $z_b$ points to the Earth center). With this orientation the first element of the quaternion is equal to 1 and the rest three are equal to zero. The velocity initial conditions are zero. It is assumed that the initial position of the system is known with some error. In the S-function for simulation of the exact body motion the initial position is set as

$$P_x = 5 \text{ m}, \ P_y = -10 \text{ m}, \ P_z = -7 \text{ m},$$

while in the EKF the same initial values are taken as zeros. The accelerations are set in the Earth fixed reference frame, after that being multiplied by the inverse $C_{eb}$ of the direction cosine matrix in order to obtain the input acceleration in the body fixed reference frame. This allows the input of accelerations to the system which correspond to the realistic trajectories in the Earth fixed reference frame.

The simulation of the navigation system work is done for angular rates

$$\omega_x = 3\frac{\pi}{180}\sin(0.01t), \ \omega_y = 3\frac{\pi}{180}\sin(0.01t), \ \omega_z = 3\frac{\pi}{180}\sin(0.01t)$$

and the linear accelerations in the Earth fixed reference frame

$$a_x = \begin{cases} 0.02, & 0 \le t < 200 \\ -0.02, & 200 \le t < 400, \\ 0.02, & 400 \le t < 600 \end{cases} \ a_y = \begin{cases} 0.01, & 0 \le t < 200 \\ -0.01, & 200 \le t < 400, \\ 0.01, & 400 \le t < 600 \end{cases} \ a_z = 0.0001$$

during a period equal to 600 s.

In Figs 4-7 we show the variation of the quaternion elements as functions of time in case of using EKF (denoted by "INS") and in case of exact measurements (denoted as "Accurate"). Clearly, after a short transient response these elements are computed with sufficient accuracy.
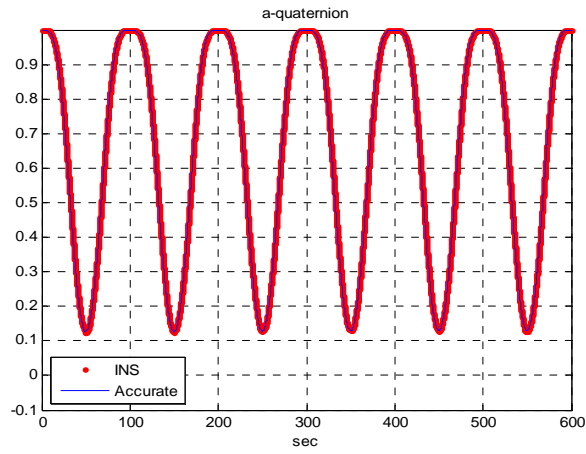
Fig. 4. Variation of the first quaternion element and its estimate
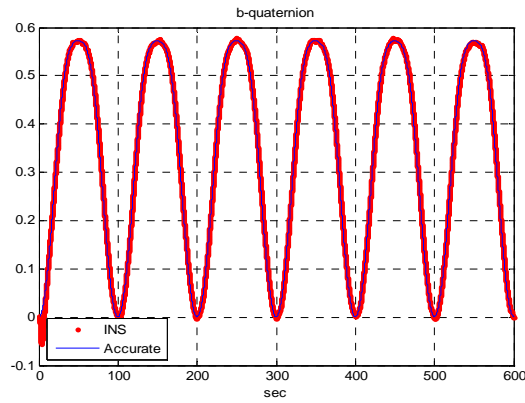


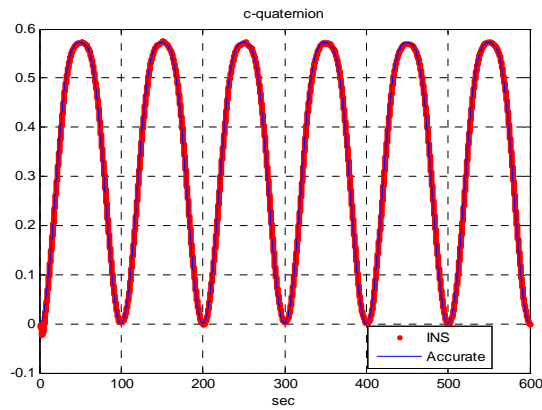Fig. 5. Variation of the second quaternion element and its estimate



Fig. 6. Variation of the third quaternion element and its estimate

In Figs 8-10 we show the errors in estimating the angular position of the body in case of using EKF (denoted by "INS") and in case of using only the noisy MEMS measurements (denoted by "NOISY"). After some initial errors due to the

16

initial conditions errors, the estimate errors in the case "INS" become very small, while those in the case „NOISY" increase significantly along with time.
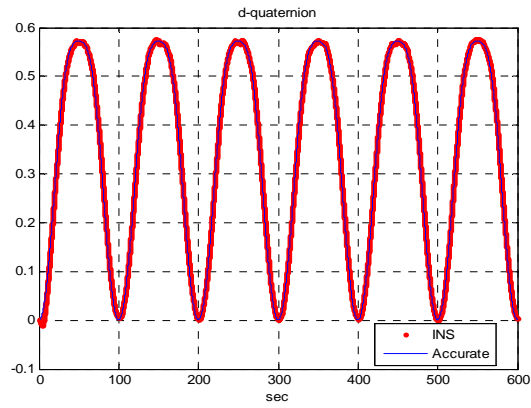


Fig. 7. Variation of the fourth quaternion element and its estimate
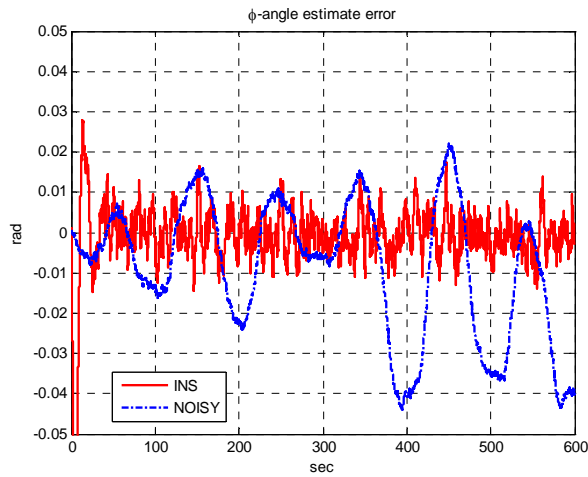


Fig. 8. Error of the roll angle estimate
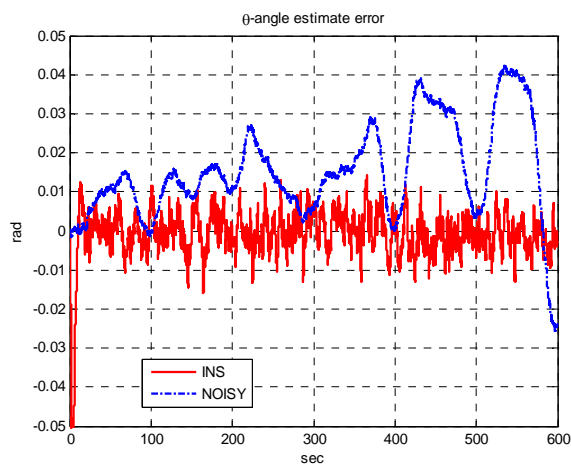


Fig. 9. Error of the pitch angle estimate

17
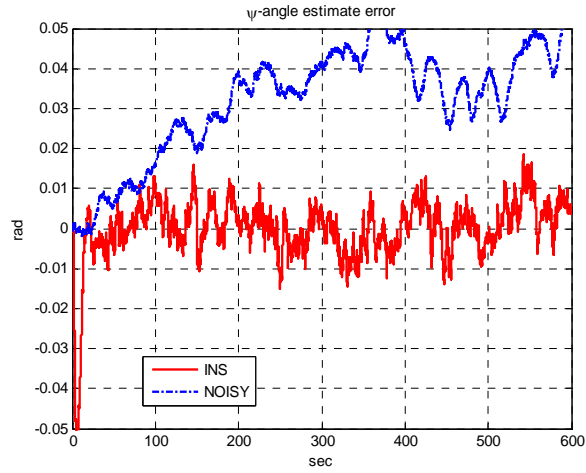
Fig. 10. Error of the yaw estimate

In order to characterize more precisely the error stochastic processes in the estimation of Euler angles we compute their means and standard deviations. The mean $m_e(k)$ at $k$-th sample is determined as

$$(37) \qquad m_e(k) = \frac{k-1}{k} m_e(k-1) + \frac{1}{k} e(k),$$

where $e(k)$ is the estimation error of the corresponding parameter.

In Figs 11-13 we show the means of the estimate errors of Euler angles for the cases „INS" and „NOISY". It is seen from the figures that after some time, depending on the initial condition errors, the error means in case „INS" tend to zero (EKF is producing unbiased estimates), while those in the case „NOISY" are divergent.
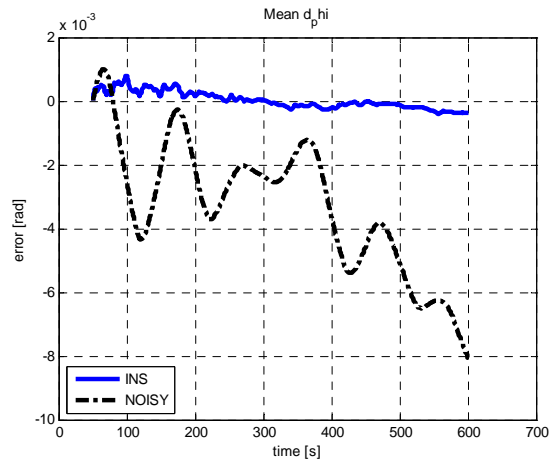


Fig. 11. Mean value of the roll angle estimate error

18
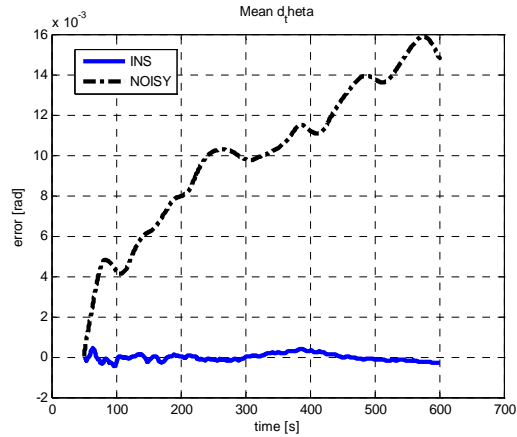
Fig. 12. Mean value of the pitch angle estimate error
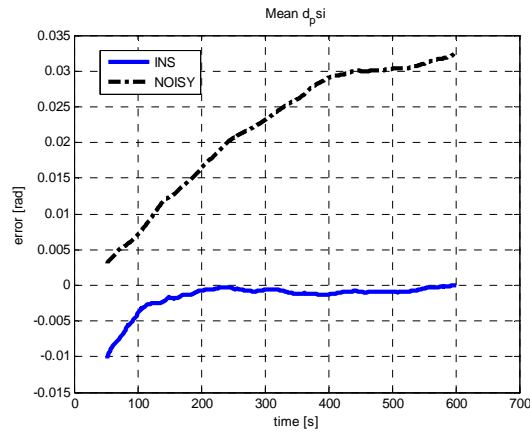


Fig. 13. Mean value of the yaw angle estimate error

The standard and maximum deviations of the errors are shown in Table 2.

Table 2. Standard and maximum deviations of the errors in Euler angles (in radians)

| Deviation | Roll angle | | Pitch angle | | Yaw angle | |
|---|---|---|---|---|---|---|
| | INS | NOISY | INS | NOISY | INS | NOISY |
| Standard deviation | 0.0049 | 0.0171 | 0.0046 | 0.0124 | 0.0055 | 0.0125 |
| Maximum deviation | 0.0132 | 0.0439 | 0.0160 | 0.0424 | 0.0187 | 0.0651 |

The results show that the standard and maximum deviations for the case „INS" are 3-4 times smaller than those in the case „NOISY".

In Figs 14-16 we show the exact positions (denoted as „Acurate") and their estimates, obtained by "INS", "NOISY" and GPS sensor. It is seen that "INS" gives very good estimates. For 10 min only "NOISY" accumulates significant errors in the position estimate, for instance the error along $z$-axis is about 400 m. Since the zero position corresponds to the Earth surface, such an error means that the navigation system based only on MEMS measurements would indicate that the body is 200 m beneath the surface.
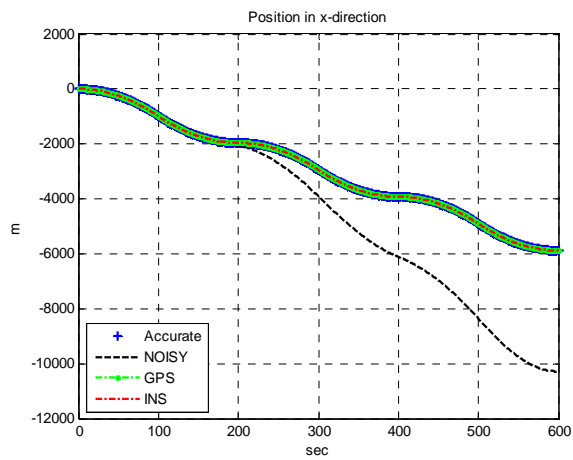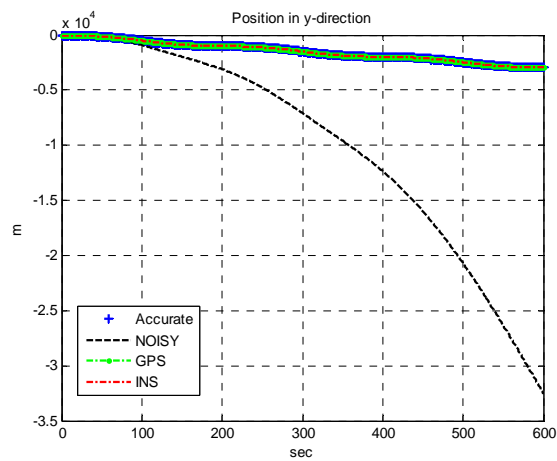
Fig. 14. Estimate of the position along *x*-axis
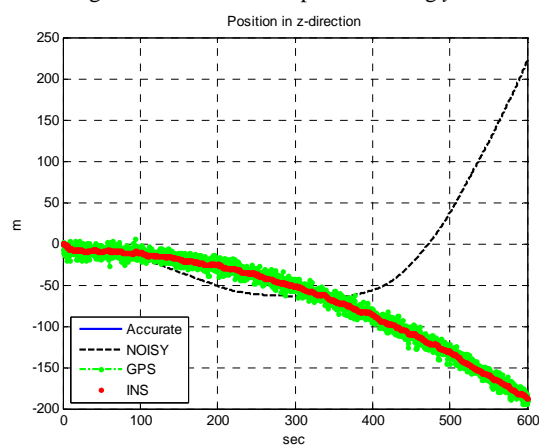


Fig. 15. Estimate of the position along *y*-axis



Fig. 16. Estimate of the position along *z*-axis

20

In Figs 17-19 we show the estimation errors in the position determined by "INS" and "GPS", the results for "NOISY" being not shown for better visualization. Clearly, the errors for "INS" are significantly smaller than those for "GPS".
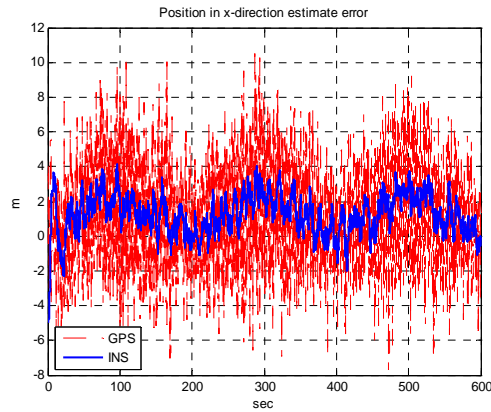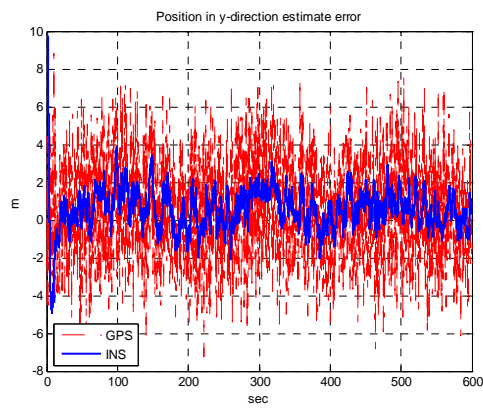
Fig. 17. Errors of position along *x*-axis estimate
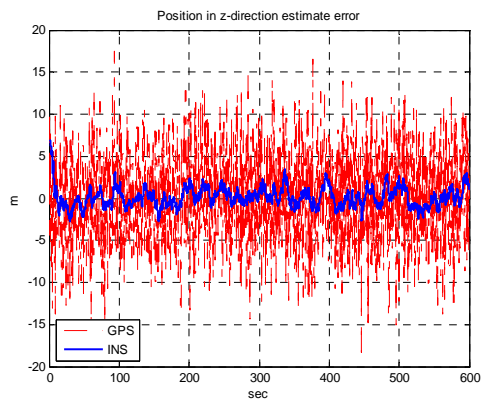
Fig. 18. Errors of position along *y*-axis estimate

Fig. 19. Errors of position along *z*-axis estimate

In Figs 20-22 we show the mean values of the errors in position estimates, computed by using the expression (37). It is seen that after the initial setting, the error mean value of the position estimate for "INS" is very close to this for the "GPS" sensor. This is to be expected, since EKF corrects the position on the basis of the GPS sensor signal.
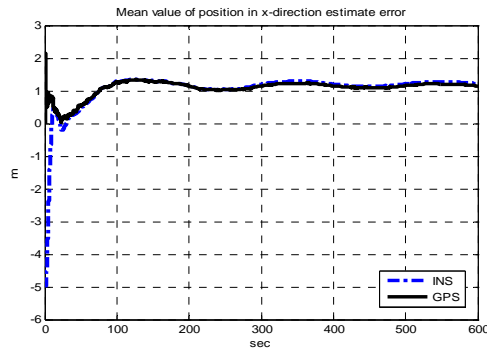


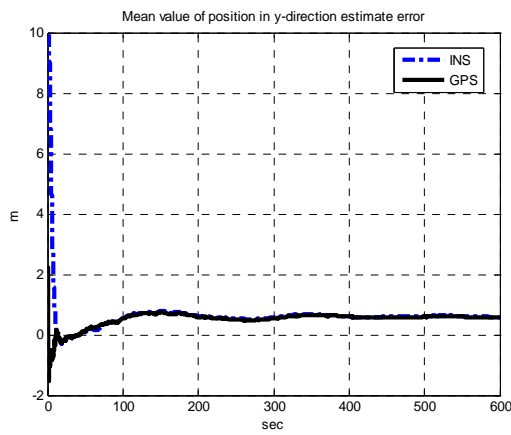Fig. 20. Mean value of position along *x*-axis estimate error



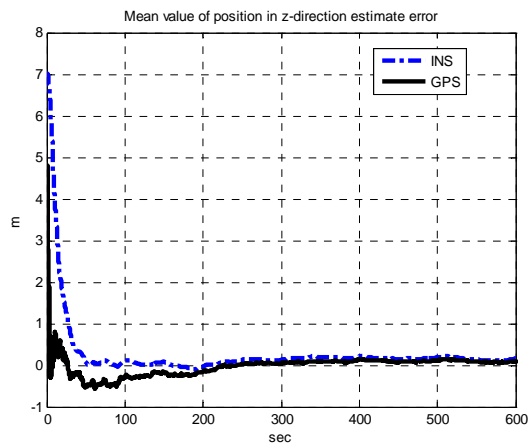Fig. 21. Mean value of position along *x*-axis estimate error



Fig. 22.  Mean value of position along *z*-axis estimate error

22

In Table 3 we show the standard and maximum deviations of the position estimate errors for "INS" and "GPS". The deviations for "INS" are several times smaller than those for "GPS". This may be explained by the fact that the errors in GPS estimates play the role of output noise in the EKF algorithm and the basic function of EKF is to reject this noise.

Table 3. Standard and maximum deviations of the errors in position estimates, *m*

| Deviation | Position along x-axis | | Position along y-axis | | Position along z-axis | |
|---|---|---|---|---|---|---|
| | INS | GPS | INS | GPS | INS | GPS |
| Standard deviation | 1.0268 | 2.4321 | 0.9207 | 2.3196 | 1.0424 | 5.0290 |
| Maximum deviation | 4.1530 | 10.4987 | 3.8644 | 8.8379 | 3.4454 | 18.3583 |

## 8. Conclusions

An algorithm for a strapdown inertial navigation system based on improved error model of the IMU ADIS16405 and aided with a GPS and magnetometer measurements is developed. The algorithm efficiency is tested by simulation. For this aim a software environment in the MATLAB/Simulink is developed which is in a form convenient for automatic generation of a code for the Texas Instruments Digital Signal Controller TMS320F28335. The simulation results show the advantage of the algorithm proposed in the attitude and position estimation over the algorithms based only on MEMS or GPS measurements. Unbiased estimates of the attitude and position are obtained which show that the Euler angle estimates are determined with errors having standard deviation less than 0.35° and the position is determined with errors having standard deviation less than 1.5 m.

## References

1. Analog Devices. ADIS16400/ADIS16405: Triaxial Inertial Sensor with Magnetometer.
   **http://www.analog.com**
2. F a r r e l , J . A . Aided Navigation: GPS with High Rate Sensors. New York, McGraw Hill, 2008.
3. G r e w a l , M . S . , A . P . A n d r e w s . Kalman Filtering: Theory and Practice Using MATLAB. 2nd Ed. New York, John Wiley and Sons, Inc., 2001.
4. G r e w a l , M . S., L . R . W e i l l , A. P. A n d r e w s . Global Positioning Systems, Inertial Navigation and Integration. 2nd Ed. Wiley-Interscience, 2007.
5. IEEE Std 952-1997. IEEE Standard Specification Format Guide and Test Procedure for Single-Axis Interferometric Fiber Optic Gyros. IEEE Aerospace and Electronic Systems Society, 1998.
6. NOAA, National Geophysical Data Center, Earth's Magnetic Field Calculators.
   **http://www.ngdc.noaa.gov/geomag/magfield.shtml**
7. P e t k o v , P . , T . S l a v o v . Stochastic Modeling of MEMS Inertial Sensors. – Cybernetics and Information Technologies, Vol. **10**, 2010, No 2, 31-40.
8. S c h i n s t o c k , D . E . GPS-Aided INS Solution for OpenPilot.
   **http://www.openpilot.org**
9. T i t t e r t o n , D., J . W e s t o n . Strapdown Inertial Navigation Technology. 2nd Ed. The Institutionof Electrical Engineers, UK, 2004.